RESEARCH ARTICLE **ISSN 2738-9898 (Print) ISSN 2738-9901 (Online)**

Optimization of Corona Ring for 230 kV Polymeric Insulator Using Numerical Method Combined with Statistical Approach and Different Optimization Techniques

Saurav Thapa*, Ananta Adhikari and Rammani Adhikari

School of Engineering, Faculty of Science and Technology, Pokhara University, Nepal

* Author to whom correspondence should be addressed; E-Mail: *sauravthapa4444@gmail.com*

Received : 15 November,2024; Received in revised form : 06 December 2024; Accepted : 10 December, 2024; Published: 31 January, 2025

Abstract

The key factor governing the long-term reliability of high-voltage composite insulators is electric field distribution. However, when exceeding thresholds and applied for long periods, electric field stresses under severe pollution conditions could lead to deterioration and degradation of the housing materials and consequently lead to failures of the composite insulators. High electric field stress near the energized end fitting results in a corona discharge, mainly leading to the composite insulator's aging. At the critical zone, the electric field strength can be lowered to an acceptable value by different approaches and among them installing a corona ring is considered an effective way. This research is intended to study the electric field distribution across clean and polluted insulator and to design optimized corona ring that improves the electric field stress near the triple junction point (i.e. junction between polymeric shed, surrounded air, and energized end fitting). Finite Element Method is combined with MATLAB in-order to obtain different critical electric field stress at triple junction point for different corona ring configuration. Based on the result from different configurations, optimization function is generated using statistical approach i.e. using MINITAB, which is then further optimized using different optimization techniques (Particle Swarm Optimization, fmincon and Runge Kutta Method). The optimized design parameters are validated with the implementation of the Finite Element Method for the clean and polluted (uniform and non-uniform) insulator resulting 58.852.% and 54.48% reduction of electric field stress for normal and non-uniform pollution condition compared to recommended corona ring.

Keywords

Electric field, Finite Element Method, Corona ring, Polymeric insulator

1. Introduction

Insulators are dielectric materials that are generally utilized in power systems for the double purpose of electrically isolating and mechanically supporting the live phase conductors from grounded towers. The insulator is an essential part of the power system which plays a significant role in sustaining the reliability, and performance of the system. Insulators in power lines are exposed to different natural phenomena and have to operate in all abnormal conditions. They have to withstand over voltages from lightning and other events and also from different environmental conditions such as rain, snow, UV radiation, and many more [1].

In modern days with the enhancements in manufacturing and design, utility companies around the world are progressively interested in using polymeric insulators. These

insulators were announced in 1959 and after the outline of polymeric insulators, the honor to use it as a spare for glass and ceramic has extremely surged worldwide. Polymeric insulators are considerably lightweight and easy to handle. Due to their lightweight nature, installation and maintenance is easy. They can be built with larger heights compared to ceramic insulators; the height can be made larger but the only constraint is difficulty in transportation with an increase in height. It provides higher mechanical strength and tracking resistance and performs better during different environment condition due to its hydrophobic properties makes its suitable for polluted regions [2].

The research of the electric field on polymeric insulators when subject to high voltage delivers a significant insight into the progress of the insulator's performance. Also, a corona ring's design plays a vital role in the insulator's performance. The corona ring diminishes the electric field by redistributing it more uniformly over a larger area, smoothing out sharp edges or points where the field would otherwise be concentrated. Corona rings are suggested on both the earth and high voltage sides of the insulator string at voltages above 345 kilovolts and only at the HV side in the voltage range between 230 and 345 kV However, for the usage of corona ring there are no any specific guideline governing the positioning and design of corona ring so each manufacturer has their own guidelines [3]. Figure 1 shows the corona ring geometry in presence of insulator.

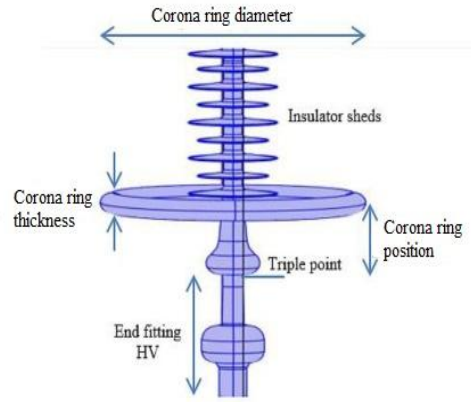

Figure 1: Corona Ring Geometry

Due to the complex geometry of insulators along with the corona ring, the calculation of electric field and even voltage distribution was a hard thing to do but using modern numerical techniques, the complex geometry can be comparatively easily modeled and simulated. For the calculation of the electric field and potential distribution based on FEM (Finite Element Method) a numerical simulation is used. COMSOL Multiphysics can be served as an interactive and powerful method to solve complex problems via the FEM [4]. As FEM is one of the utmost successful means to resolve electrostatic problems via the discretization of the domain, it is most appropriate to compute the electric field and potential distribution in high-voltage insulators. Besides FEM there are different techniques for estimating potential distribution and electric field such as Charge Simulation Method (CSM), Finite Difference Method (FDM), and Boundary Element Method (BEM). Many publications can be found in the evaluation of the E-field and potential distribution for high voltage insulators and different optimization methods for optimizing corona ring parameters. In [5] FEM analysis of electric field distribution for clean insulator is conducted which identifies of vulnerable areas of insulator units where damage and consequent breakdown may occur. From the results presented the most critical

areas for the insulator is triple junction point i.e. in case of porcelain insulator it's the junction between the (pin-cement, cement-porcelain/glass) of the bottom disc insulator unit. Paper [6] described the effect between electric field distribution and flashover voltage. Around 6 several different ceramic and composite insulators were used to determine electric field distribution with a new electric field measurement technology. Initially, the dependency between contamination layer conductivity with the environmental relative humidity was analyzed. Moreover, the electric field distribution patterns for clean, uniform, and non-uniform contamination cases were analyzed and its correlation with the flashover voltage is investigated. In [7] BP neural network was applied to handle the optimization of corona ring on composite insulators. The optimization neural network model is built which solves the problem of long computing time of the exhaustive method. Then, an optimal scheme of the structure parameters of 330 kV composite insulators is obtained. After optimization, the results display that, the surface field strength of the corona ring and the insulator field strength along the surface are all less than the corona's initial field strength i.e., 4.5kV/cm. Seven cases of polymer insulators with alternate sheds were considered in [8] using the weighted sum technique for resolving the multi-objective optimization issue. The E-field distribution on composite insulators with the areas close to the energized is non-linear and usually is exposed to the highest magnitudes. In the technique an adaptive meshing algorithm was applied that ensures the lesser numerical faults and a stables performance of optimization algorithm. Dynamic Population size concept is introduced in [3] for the optimal design of corona ring by means of PSO.

Different optimization toolbox from MATLAB (fminbnd, fmincon, Optimtool-Genetics Algorithm) is used for optimization process in [9], combined with FEM using two different ways. Firstly, the housing material shape and permittivity were taken as optimized parameter and in second case the dimension and position of corona ring were considered as optimization parameter with an overall aim to reduce electric field across insulator. Paper [10] has achieved a shape optimization of a high voltage insulator in three steps; firstly, a finite element method is used to determine tangential electric filed. Secondly, a data base was created to determine objective function and finally in third step genetic algorithm was used to determine optimized parameter. The objective of shape optimization is to reduce the tangential electric field stress along the surface of polluted insulator. In [11] the performance and comparison of different multi-objective meta-heuristic algorithms namely, 'MOPSO' (Particle Swarm Optimizer), 'NSGA-II' (non-dominated sorting genetic algorithm) and 'MOALO' (Ant Lion Optimizer) to improve the electric field distribution and potential for 400 KV composite insulator is presented which results MOPSO gives better electric field distribution and a reduction of about 55% and 75% in computational time was obtained using MOALO. The electric field using FEMLAB (old version of COMSOL Multiphysics) and MATLAB built-in optimization function in [12] results that with the change in dimension and positioning of corona ring the maximum electric field also keeps on changing i.e. electric field is not always at specific point so the objective function is more complex and is specified as the maximum of field along the axial length of insulator. In [13], an analysis of the behavior of the electric field and the potential for three different types of insulators, the glass, the

porcelain and the polymeric is presented in presence of pollution. Despite the presence of the pollution layer the values of the electric field remains below the dielectric strength of the air. The pollution layer reduces the contribution of the electric field which can be explained by the point effect i.e. as the pollution layer rounds the ends of the sheds of the insulators the electric field will then be lower. A uniform contamination of the insulator is therefore beneficial for the insulator, unlike a discontinuous contamination.

Different methods, optimization techniques can be implemented to reduce the electric field stress near the high voltage side of the insulator which could be achieved by improving the insulators shed configurations or by optimizing corona ring parameters. However, in order to determine the field distribution, FEM analysis is mostly used as it allows discretization of domain. This research is focused on optimizing corona ring parameters using FEM combined with the statistical approach and different optimizing techniques.

2. Methodology

2.1 Insulator under study

The study was conducted using a real world 230 kV polymeric insulator with the following geometric characteristics [14] shown in Table 1 and Table 2 along with the corona ring. In this case the manufacturer considered the corona ring with dimensions as corona ring diameter was 305 mm, the ring tube diameter was 30 mm, and the position regarding end fitting was 155 mm from the HV end of corona ring. The insulator and corona ring were designed in AutoCAD as shown in Figure 2. In addition, pollution with thickness 2mm was also designed as shown in Figure 3 where it consists of two models of pollution i.e. uniform and non- uniform pollution. For the study of field distribution along the insulator the simulation was carried out using COMSOL Multiphysics 6.2 software.

Table 1 Dimension of 230KV Polymeric insulator

Total length between end fittings	8475mm
Total leakage distance	2556.544mm
Number of large sheds	30
Number of small sheds	29
Large shed diameter	164mm
Small shed diameter	132mm

Table 2 Dimension of Corona Ring

Corona Ring Diameter	305mm
Ring Tube Diameter	30mm
Corona Ring Position	155mm

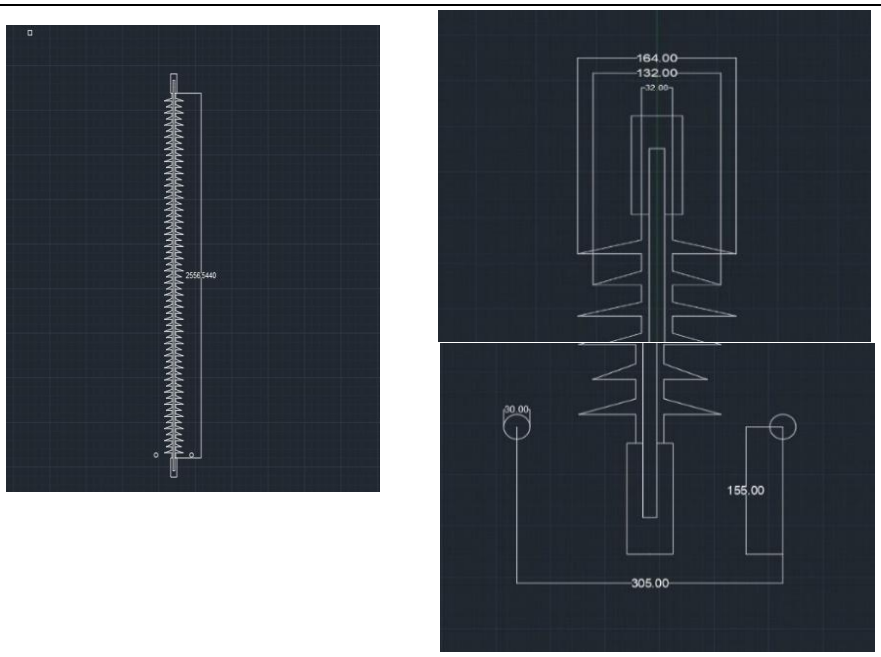

Figure 2: 2D geometric model of 230KV insulator with corona ring

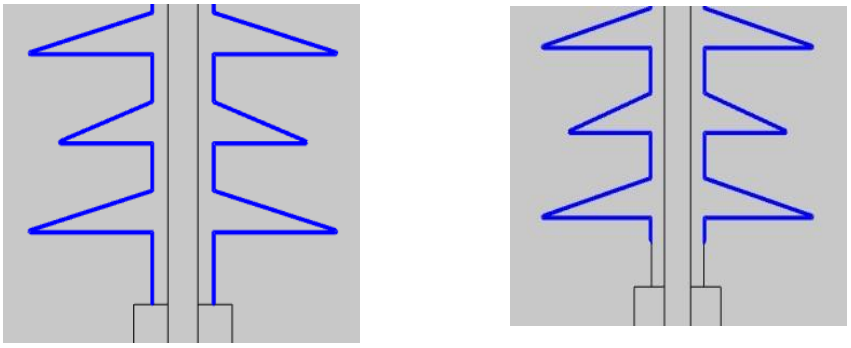

a)Uniform Pollution b) Non-uniform pollution

Figure: 3 Polymer insulator with pollution layer model

2.2 Boundary Condition

A 230 kV alternating current voltage energized the HV conductor at 50Hz. The connection between the energized end fitting attached to the conductor and corona ring was energized at 230 kV whereas the connection between the end fitting to the tower arm was modeled to be at ground potential i.e. 0 volts. And the insulator was surrounded with the air space. The overall boundary condition being used to model the insulator along with corona ring is shown in Table 3 and Table 4 whereas; the overall model in COMSOL Multiphysics seems as Figure 4.

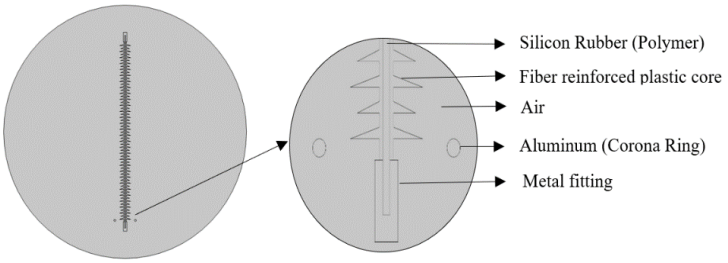

Figure 4: Polymer Insulator modelling in COMSOL Multiphysics

Table 3: Properties of material used in simulation [14]

Material	Component	Relative Permittivity	Conductivity (S/m)
Fiberglass	Fiberglass rod	5.5	1e-12
Silicon	Polymeric sheds	3.2	1e-17
Steel	End Fitting	1.0	1.7e6
Aluminum	Corona ring	1.0	3.8e7
Air	Working region	1.0	0
Pollution	Working region	81.0	0.001

Table 4: Boundary of the electric field [14]

Boundary	Boundary Setting
Terminal	Applied voltage 230 KV
Air	Electric Insulation
Ground	0V
All interior boundary	Continuity

2.3 Electric Field Calculation Equation

Electric field and potential distribution calculation on HV insulator are useful in studying the behavior of insulator in different condition.

The electric field is defined as the negative gradient of the electric potential [15], given by:

$$E = -\nabla V \quad (1)$$

Gauss's law, one of Maxwell's equations, relates the electric flux to the charge density. As detailed in [15], this relationship can be expressed mathematically as:

$$\nabla . E = \frac{\rho}{\varepsilon} \quad (2)$$

Substituting the value of Electric field (E) in equation (2),

$$\nabla.(-\nabla V) = \frac{\rho}{\varepsilon} \quad (3)$$

Where, ρ is the charge density and $\varepsilon = \varepsilon_0 \varepsilon_r$, where ε_0 is the permittivity of air and ε_r is the relative permittivity of insulating material. Starting with Gauss's law (Equation 2), and substituting the electric field as the gradient of the potential, we obtain Poisson's equation.

$$\nabla^2 V = -\frac{\rho}{\varepsilon} \quad (4)$$

When the surface charge ρ =0 then the Laplace's equation can be derived as,

$$\nabla^2 V = 0 \quad (5)$$

However, continuity equation needs to be considered while evaluating the electric field distribution along insulator's contaminated surface expressed as [5].

$$\nabla. \left(J + \frac{\partial D}{\partial t}\right) = 0 \quad (6)$$

Where, J is the current density (A/m^2) given by $J = \sigma E$ and $D = \varepsilon E$, where σ is electric conductivity (S/m^2), then equation (2.6) can be written as,

$$-\nabla(\sigma \nabla V) - \nabla\left(\varepsilon \nabla \frac{\partial V}{\partial t}\right) = 0 \quad (7)$$

In case of DC, the partial derivative term becomes zero and equation (7) will be,

$$-\nabla(\sigma \nabla V) = 0 \quad (8)$$

From equation (2.8) we can see that the Electric field distribution under contaminated condition depends upon the value of electrical conductivity σ.

For 2-D, the equation of the place in Cartesian coordinates is given by,

$$\nabla^2 V = \frac{\partial^2 V}{\partial x^2} + \frac{\partial^2 V}{\partial y^2} \quad (9)$$

2.4 Statistical Approach

The mathematical relationship between the corona ring parameters (ring radius, ring height and tube radius) and the electric field strength builds up the objective function given as:

F = E (ring radius, ring height, tube radius), where, each parameter has physical constraints i.e. upper and lower limit. The relationship between the electric field strength and corona ring parameters were related with second degree polynomial line based on FEM results. Through the polynomial line, model was derived and to assess the accuracy of model, coefficient of determination (R^2) was used. If R^2 was equal to or greater than 0.6 the models were adequate. The model was obtained for triple junction point considering every different design parameter: ring radius, ring height and ring tube radius. The function in triple junction point was considered as the average of E (ring radius), E (ring height), and E (tube radius).

F_t = (E (ring radius) + E (ring height) + E (tube radius))/3 (10)

In order to get the electric field for different corona ring configuration; COMSOL Multiphysics was linked with MATLAB. The objective function was developed using electric field data (variation in ring radius, tube radius and ring height), which demonstrates the close relationship with the simulation result. The residual analysis assesses the accuracy of regression models by examining the differences between model and simulated values and provides information about the adequacy of the model. For that we check if residuals are approximately normally distributed or not.

2.5 Optimization Process

2.5.1 Particle Swarm Optimization

PSO is a computational method used to find the optimal solution to the problem. This algorithm is inspired from the relationship of travelling birds and the way they optimize their movements when travelling long distance searching for foods. In search of food, they continuously update their position and in respect to their own best position and best position of entire population i.e. swarm and regroup themselves towards optimal formation. In order to optimize continuous non-linear function in 1995, James Kennedy, a social psychologist and Ruseell Elberhart, an electrical engineer developed PSO which works on iteration [16]. This algorithm starts with population named as swarm representing the group of birds. Each particle (bird) in search of food represents the position and velocity in order to solve the given problem. For each iteration, all particles representing the population keeps on updating the position and velocity. Each iteration has its own global best (gbest) value and personal best (pbest) value. Global best value represents the best position for entire iteration i.e. the best position is influenced by the best position found by any member of the entire population whereas personal best value represents the best position for each particle. These best values keep on updating with each iteration i.e. the best position keeps on updating. And therefore, each particle position will converge to the new position until the optimal solution is obtained from the solution space. The flowchart for the Particle Swarm Optimization (PSO) algorithm is presented in Figure 5 [17].

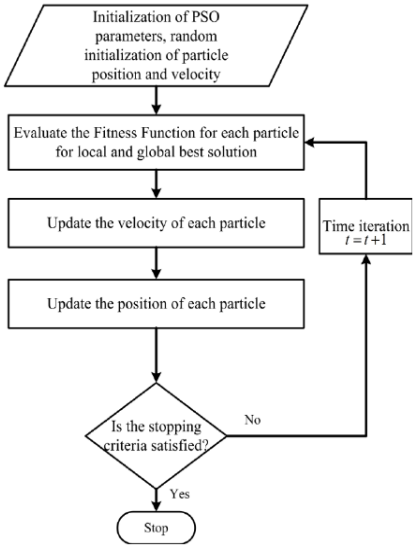

Figure 5: Flowchart for Particle Swarm Optimization [17]

2.5.2 FMINCON

fmincon is a MATLAB function that is used to find the minimum of a constrained non-linear multivariable function. It is a gradient-based function that can be used to search and find all different local minima that meet the set of objectives [18]. It all starts with an initial guess based on an algorithm and goes on until all setup criteria are met. If all the requirement of 1st order optimization is met by the last iteration, the conclusion is considered as a local minimum that fulfills the system's needs. fmincon has different algorithm options: (a) Interior point (b) Trust – region – reflective (c) Active Set (d) SQP (Sequential Quadratic Programming).

2.5.3 Runga Kutta Method

The integration of the Runge-Kutta 4 (RK4) technique with gradient descent can produce strong iterative optimization procedure, where RK4 improves the parameter updates according to gradient of the function. The RK4 method is typically used to solve differential equations but will be used here to calculate the next point in parameter space based on gradient information [19].

Algorithm: RK4 Gradient Descent

1: Input: Objective function f(x), initial guess x_0, learning rate α, max iterations max_iter, convergence threshold ϵ.

2: Output: Optimal solution $x_{optimal}$ and minimum function value $min_f=f(x_{optimal})$.

3: Initialize: Set $x= x_0$, iteration counter k = 0.

4: while k<max_iter do

4.1: Compute Gradient ∇f(x)

4.2: RK4 Updates:

- $k_1=-\alpha\cdot\nabla f(x)$
- $k_2=-\alpha\cdot\nabla f(x + 0.5\cdot k_1)$
- $k_3=-\alpha\cdot\nabla f(x + 0.5\cdot k_2)$
- $k_4=-\alpha\cdot\nabla f(x + k_3)$

4.3: Update Position $x_{new}=x+\frac{1}{6}(k_1+2\cdot k_2+2\cdot k_3 + k_4)$

4.4: Check Convergence:

- If $\|xnew-x\|<\epsilon$, stop.

4.5: Update x=xnew, k=k+1

end while

5: Output $x_{optimal}= x$, $min_f=f(x_{optimal})$

Helper Function: compute_gradient

1: Function: compute_gradient

1.1: Input: Objective function f(x), current position x.

1.2: Initialize:

- Set h=1e−5(a small step for finite differences).
- Initialize gradient vector grad as a zero vector of the

same length as x.

1.3: Calculate Gradient:

- For each dimension i:
  - Set x_1 = x and x_2 =x.
  - Compute:
    - $x_1(i)= x_1(i)+h$
    - $x_2(i)= x_2-h$
  - Update grad(i) = $\frac{f(x_1)-f(x_2)}{2h}$

1.4: Output: Return grad, the computed gradient vectors.

3. Results and Discussion

The triple junction point is considered as vulnerable region in terms of electric field stress. The simulation was focused on triple junction point where the electric field stress should not surpass the value 4.2 kV/cm, considered as critical value [20]. Initially the simulation was carried out without considering the corona ring and then considering the recommend corona ring as shown in Table 2. Without the corona ring the stress was near about 3.932 kV/cm which got reduced to 47.94% with the installation of recommended corona ring. However, in order to reduce the field stress further, so that the rate for the overall aging of the insulator decreases this research dived into the optimization of recommended corona ring parameters. And the optimized corona ring performance is been evaluate in the presence of pollution condition i.e. uniform and non-uniform pollution condition. The overall simulation and optimization process were run on a PC with an Intel(R) Core(TM) i7-7700HQ 2.67 GHz processor and 8 GB RAM.

3.1 Electric field analysis for recommended Corona Ring

At first, we study the electric field behavior for the existing corona ring parameters and then accordingly we will establish the relation between electric field and corona ring parameters.

3.1.1 Electric field distribution with and without corona ring

The simulation was first run without the corona ring, to determine the electric field strength at the triple junction site. The results in Figure 6 shows that in the vicinity of the energized-end fitting, the potential distribution leads to a high electric field strength. The maximum electric field (3.932 kV/cm) occurred on the triple junction point. It is possible to have an excess of the recommended value of the electrical field. For the transmission line running at 230KV, corona ring should be fitted on energized-end fitting as stated above. Therefore, in the subsequent simulation, a recommended corona ring has been incorporated in the energized-end fitting. Figure 7 shows the electric field strength gets significantly reduced with the installation of corona ring to value 2.047 kV/cm i.e., 47.94% reduction.

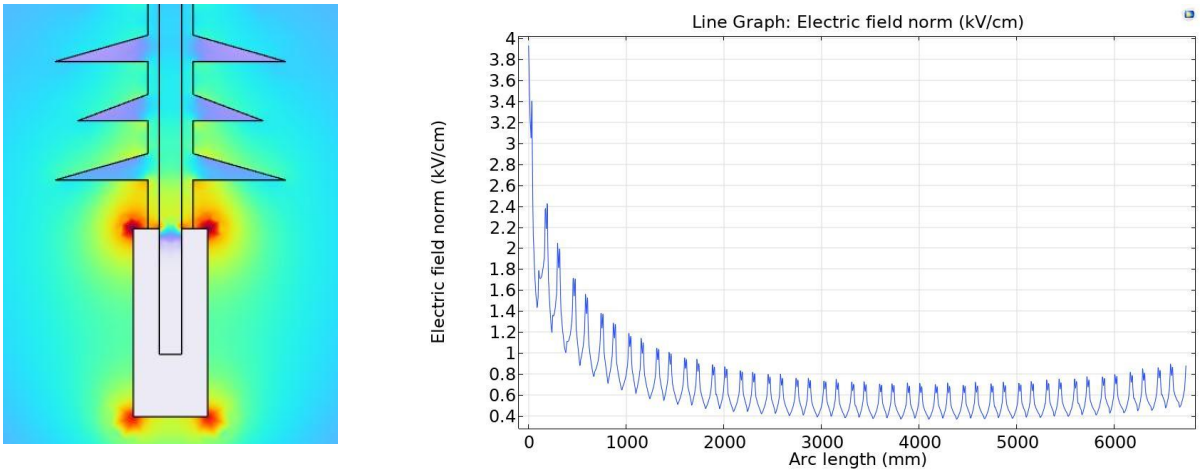

a) Contour Map b) Field Distribution

Figure 6: Electric field contour map and distribution on the energized-end fitting surface without corona ring

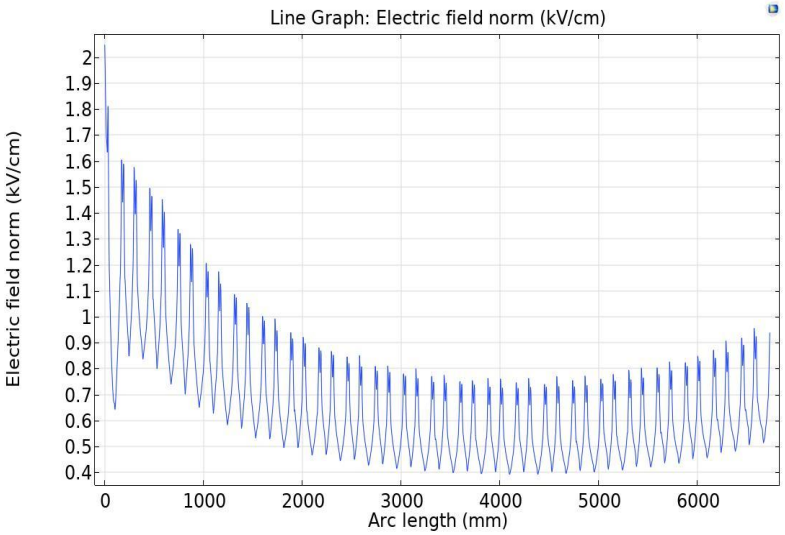

Figure 7: Electric field distribution along the creepage length with corona ring

3.1.2 Analysis and determination of corona ring parameters constraints

The variables that should be considered for optimization to reduce the electric field stress around the triple junction point are the corona ring radius (R), the corona ring tube radius (r), and the corona ring position (H). To determine how each parameter impacts towards the maximum electric filed, each parameter (R, r, H) is subjected towards the change with other parameters. Figures 8, 9, and 10 show the impacts of the mounting location (H), the radius (R) and the tube radius(r) of the ring respectively. Note that H, R and r are varied in the steps of 50mm, 50mm and 5mm respectively.

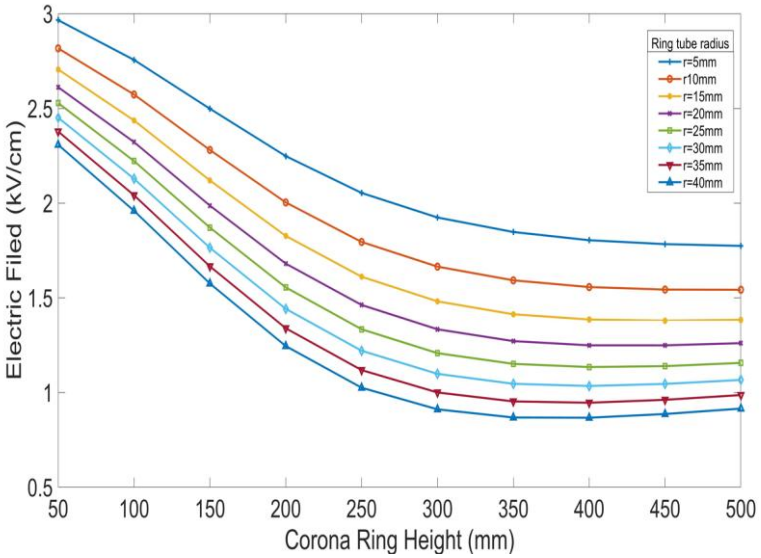

Figure 8: Maximum electric field vs corona ring height for different corona ring tube radius and ring radius = 200mm

In Figure 8, the electric field gets reduced as the height of the corona ring increased from 50 mm to 500 mm and at nearly about 300 mm the minimum value is achieved which further becomes nearly constant. Therefore, taking it into consideration the choice for the height in the range of 135 to 500 mm is appropriated in order to find the minimum value for electric field.

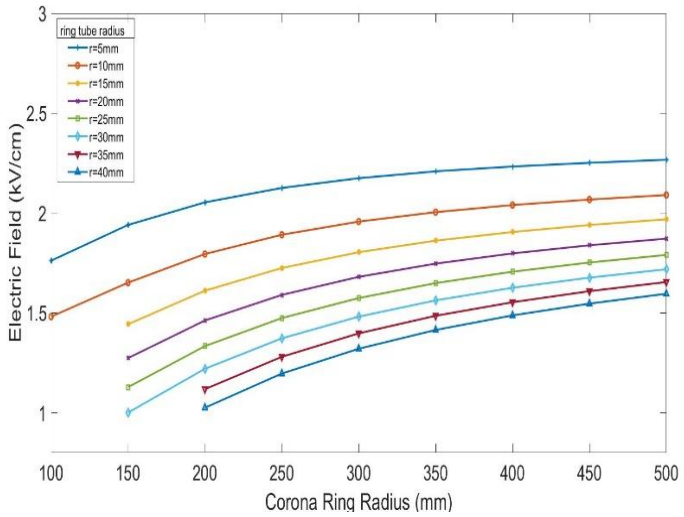

Figure 9: Maximum electric field vs corona ring radius, for different corona ring tube radius and ring height = 200 mm

Figure 9 demonstrates that the increase in the radius of the corona ring in general leads to an increase of the maximum electric field and beyond 450 mm maximum electric field is practically unaffected. To avoid the contact between the corona ring and the bigger shed the inferior limit for the corona ring radius should be greater than the larger shed radius of 82 mm. However, there is chance for ring tube radius (r) to be at maximum value 40 mm so taking it into consideration we choose corona ring inferior limit to be 200 mm. The electric field has not essentially changed for radius greater than 450 mm. So, we have set the superior limit of the ring radius at 450 mm.

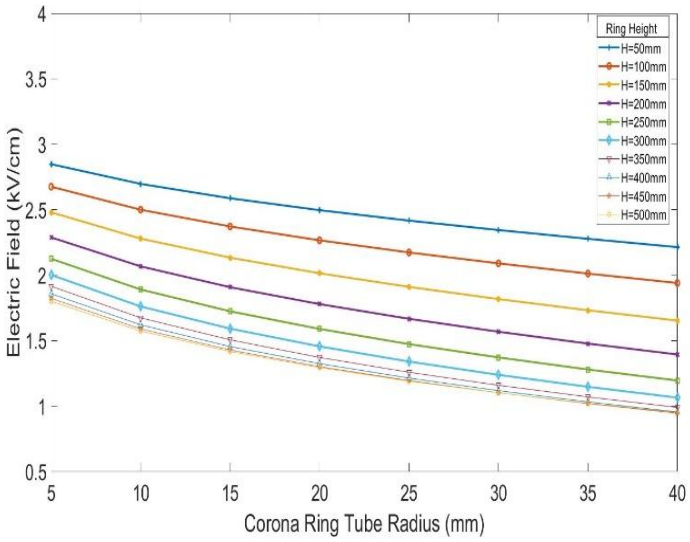

Figure 10: Maximum electric field vs corona ring tube radius, for different corona ring height and ring radius =250mm

Concerning the ring tube radius effect represented in Figure 10, high electric field is produced by a low corona ring tube radius. So, ring tube radius lower than 5mm is not appropriated and the tube radius greater than 40mm becomes larger bulkier and are not economically viable. Therefore, the inferior and superior limit for corona ring tube radius is set between 5mm and 40mm.

Analysis of figures, gives the idea regarding the variation of corona ring parameters with respect to the electric field at the triple junction point. Therefore, corona ring parameters for the further optimization process are considered as shown in Table 5.

Table 5: Range for corona ring parameters

Parameters	Original value(mm)	Range (mm)
Ring Radius	152.5	200 – 450
Ring Height	155	135 – 500
Ring Tube Radius	15	5 – 40

3.2 Electric Field Function

Based on the simulation's findings, the electric field models for triple junction point are developed. The polynomial line of order 2 was found for each series shown in Figure 11 (a,b,c). Since individual variation in each parameter resulted same trend line, so we will consider the objective function in equation 10 as the average of electric field function where two variables are kept constant, and the third one is varied in its respective range. In order to determine the electric field model MINITAB 18 was used that provide the quadratic equation for three different variation of corona ring parameters.

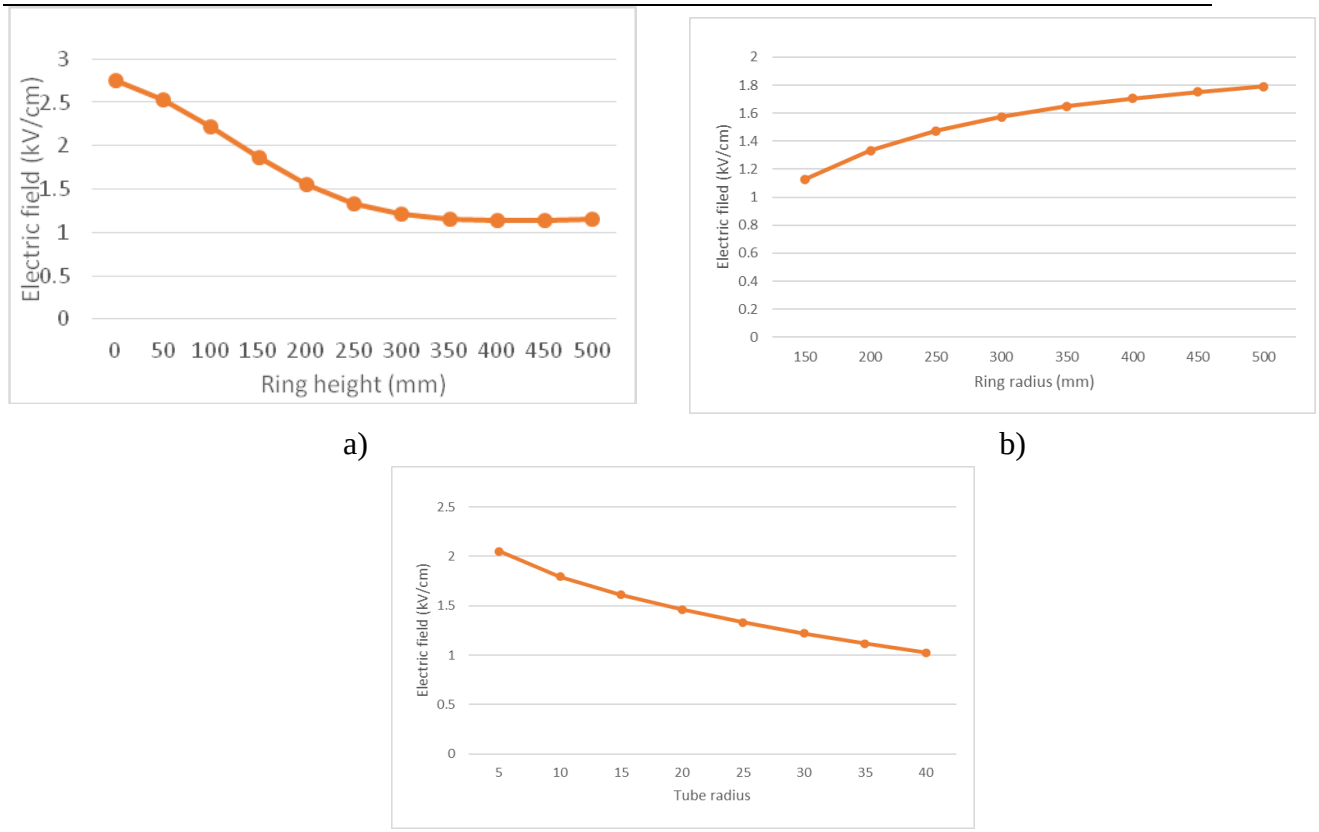

a) b)

c)

Figure 11: Electric field as a function of a) ring height (R=200mm, r=25mm) b) ring radius (H=250mm, r=25mm) and c) tube radius (H=250mm, R=200mm)

The three quadratic models for the triple junction point composed of equations 11, 12 and 13 which describe the correlation between the corona ring design parameters and the electric field at the triple junction point. For the given model, coefficient `of determination (R^2) had a minimum value of 0.9868. These equations are substituted in equation 10 get Equation 14 i.e. objective function. The coefficients of determination are summarized in Table 6.

Table 6: Coefficient of determination (R^2) of each quadratic model

Parameters Evaluated	Coefficient of determination
Ring radius (R)	0.9927
Ring height (H)	0.9868
Ring tube radius (r)	0.9967

$$E(\text{ring radius}) = -5e^{-6}\,\text{ring radius}^2 + 0.005103\,\text{ring radius} + 0.498 \quad (11)$$

$$E(\text{ring height}) = 1e^{-5}\,\text{ring height}^2 - 0.008266\,\text{ring height} + 2.852 \quad (12)$$

$$E(\text{tube radius}) = 4.74e^{-4}\,\text{tube radius}^2 - 0.04961\,\text{tube radius} + 2.267 \quad (13)$$

Therefore,

$$F_t = (-5e^{-6}\,\text{ring radius}^2 + 0.005103\,\text{ring radius} + 1e^{-5}\,\text{ring height}^2 - 0.008266\,\text{ring height} + 4.74e^{-4}\,\text{tube radius}^2 - 0.04961\,\text{tube radius} + 5.1675)/3 \quad (14)$$

Figure 12 represents the comparison between results derived from the model equation 14 and the simulated electric field strength from COMSOL Multiphysics for the 20 configurations. It is observed that the simulation values match with the calculated electric field strengths.

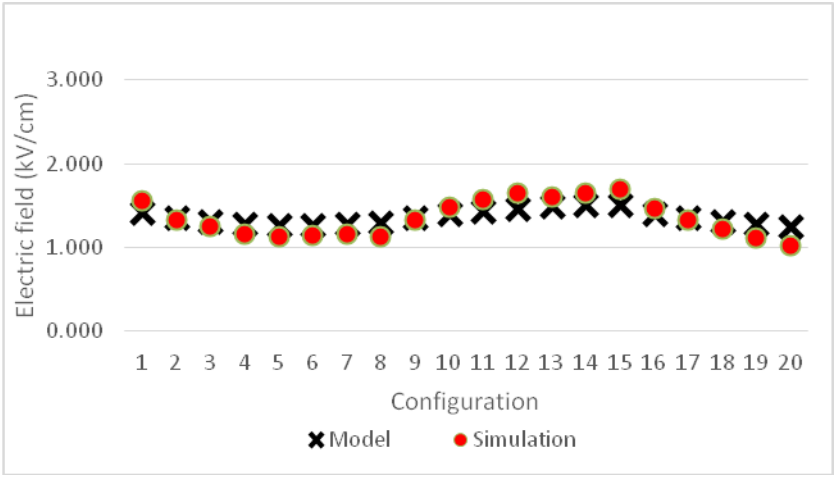

Figure 12: Comparison of the simulated electric field strength with the calculated values at triple junction point

Figure 13 shows the normal distribution probability plots with a 95% confidence level for the residuals between predicted model and simulated values. The straight line fit of the data indicates the suggested model works well as they follow a normal distribution.

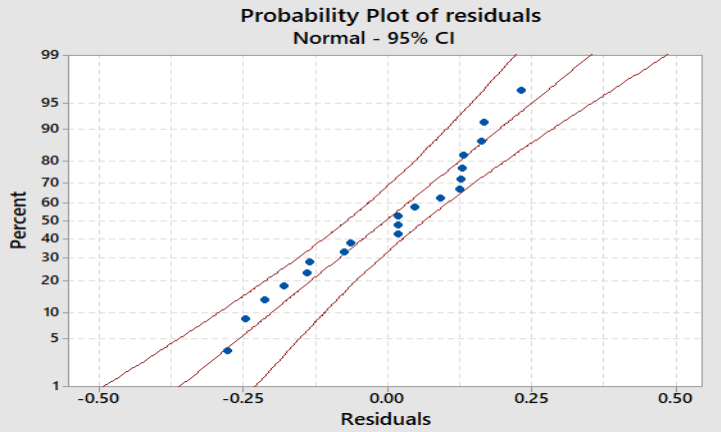

Figure 13: Normal distribution probability plots with a 95% confidence level for the electric field strength residual between simulation and model

3.3 Optimization Result

The equation for electric field function is obtained as a second-degree polynomial equation, which is optimized through various techniques. The PSO algorithm were carried out with the following configuration i.e. c1 = 1.5, c2 = 1.5, w = 0.5, swarm size = 30 and the convergence criteria was set to 1e-6. The convergence of solution deaccelerates with the larger number of swarm particles or iteration whereas with the fewer number of swarm

particles or iteration, lowers the possibility of obtaining high quality results. The optimized value is obtained at 8th iteration as shown in Figure 14 with the corona ring tube radius r = 40 mm, corona ring radius R = 200 mm and the corona ring position (height) H = 413.23 mm respectively. Therefore, in comparison to the recommended corona ring an increase of 166.6%, 31.15% and 166.6% in ring tube radius, ring radius and ring height is obtained.

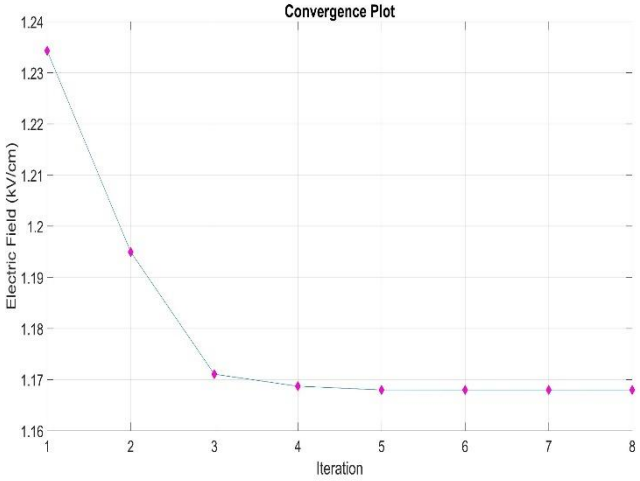

Figure 14: Convergence characteristics during the optimization process using PSO

fmincon is based on constrained nonlinear optimization or nonlinear programming models. For the given function the parameters were optimized at 15th iteration as shown in Figure 15 with SQP algorithm resulting nearly the same performance as PSO i.e. the corona ring tube radius r, corona ring radius R and the corona ring position (height) H equals to 40 mm, 200 mm and 413.3 mm respectively.

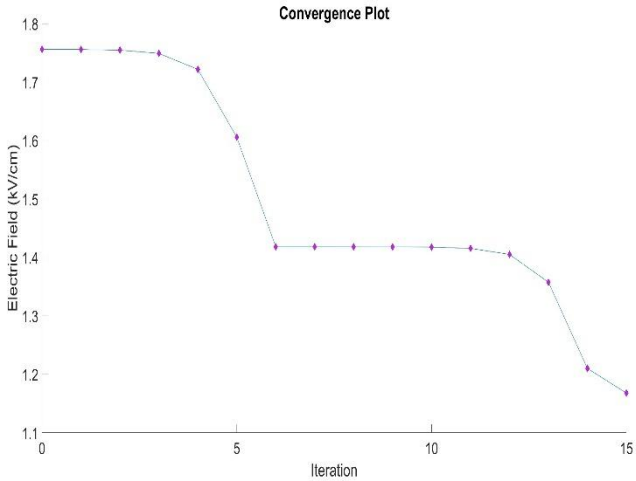

Figure 15: Convergence characteristics during the optimization process using fmincon

The convergence rate greatly depends on the step size and the number of iterations. Higher the convergence rate or the step size, objective function gets faster. Therefore, in order to optimize our multi variable nonlinear algebraic function RK algorithm were carried out with the following configuration i.e. step size = 700 and iteration = 3000. For the given function the parameters were optimized at iteration number 2032 as shown in Figure 16 resulting the same result as PSO and fmincon i.e. the corona ring tube radius r,

corona ring radius R and the corona ring position (height) H equals to 40 mm, 200 mm and 413.301 mm respectively as other optimization techniques.

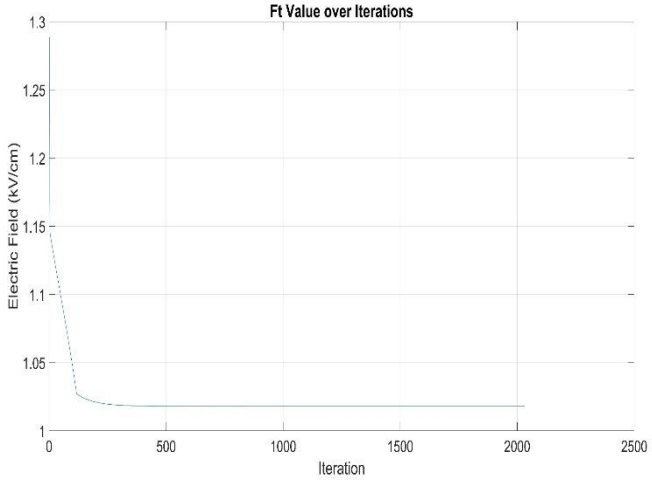

Figure 16: Convergence characteristics during the optimization process using RK method

With the optimization of corona ring parameters, the optimized parameters of corona ring are considered as shown in Table 7.

Table 7: Optimized Corona Ring Parameters

Corona Ring Radius	200 mm
Ring Tube Radius	40 mm
Corona Ring Position	413.3 mm

3.4 Electric field analysis for optimized Corona Ring

With the implementation of the optimized corona the main focus is to reduce the electric field stress at the triple junction point resulting more reliable performance of insulator with time. The electric field reduces from 2.047 kV/cm to 0.8423 kV/cm using optimized corona ring as compared to that of recommended corona ring i.e. 58.852 % reduction. As shown in Figure 17 the optimally designed corona ring not only lowers the electric field magnitude but also shifts the maximum electric field's location from the triple point as the optimized height of the corona ring is increased.

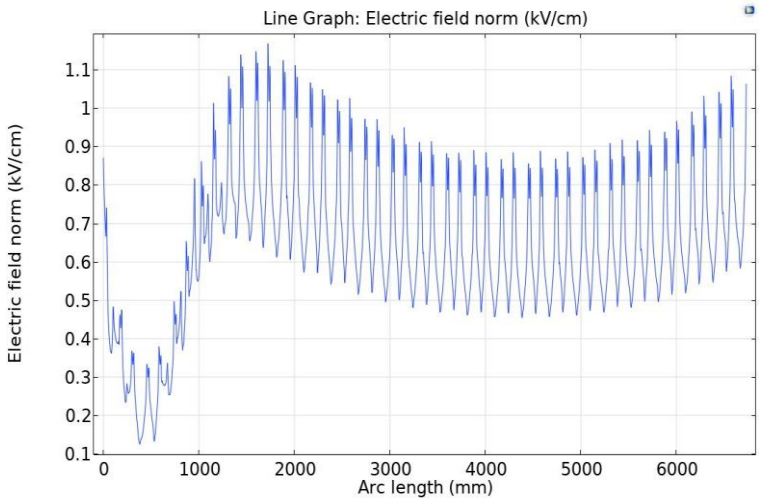

Figure 17: Electric Field analysis for optimized corona ring

3.5 Comparative Analysis

This section presents a detailed analysis of the electric field behavior of a 230 kV polymeric insulator under various conditions, including normal and polluted environments, with the use of both recommended and optimized corona rings. The findings are supported by comparative analyses illustrated in Figures 18,19 and 20.

3.5.1 Electric Field Distribution under Normal Conditions

Figure 18 illustrates the electric field distribution for normal conditions: without a corona ring, with a recommended corona ring, and with an optimized corona ring.

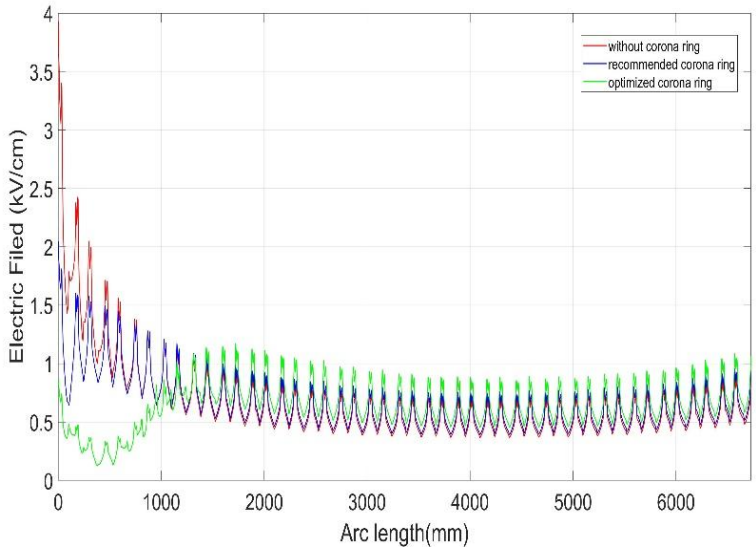

Figure 18: Comparative analysis of electric field for normal condition: without corona ring, with recommended corona ring and with optimized corona ring

The red line indicates at the start (triple junction point), the electric field is the highest, peaking around 3.932 kV/cm. This is due to the absence of a corona ring, which causes a high concentration of the electric field near the energized end. As the arc length increases, the electric field gradually decreases, but there are still noticeable oscillations throughout the length of the insulator, indicating an uneven distribution of the field. The blue line shows the electric field distribution when a standard (recommended) corona ring is used. The initial peak is lower than in the case without a corona ring, reducing to about 2.047 kV/cm. This reduction indicates that the corona ring is effectively redistributing the electric field, reducing the peak intensity near the energized end. However, there are still oscillations along the insulator length, and as the arc length increases the electric field is also slightly greater compared to without corona ring. The green line represents the electric field distribution when an optimized corona ring is applied. The initial peak is significantly reduced compared to both the "without corona ring" and "recommended corona ring" scenarios, reaching below 0.8423 kV/cm. This indicates that the optimized corona ring is more effective at reducing the electric field concentration near the energized end. Additionally, the optimized corona ring shifts the maximum electric field away from the triple junction point because as the corona ring height increases the voltage associated with also

shifts to higher region. The electric filed strength is slightly higher along the insulator compared to that normal condition with the use of optimized corona ring.

3.5.2 Electric Field Distribution under normal and pollution condition

Figure 19 compares the electric field distribution under normal conditions, uniform pollution, and non-uniform pollution.

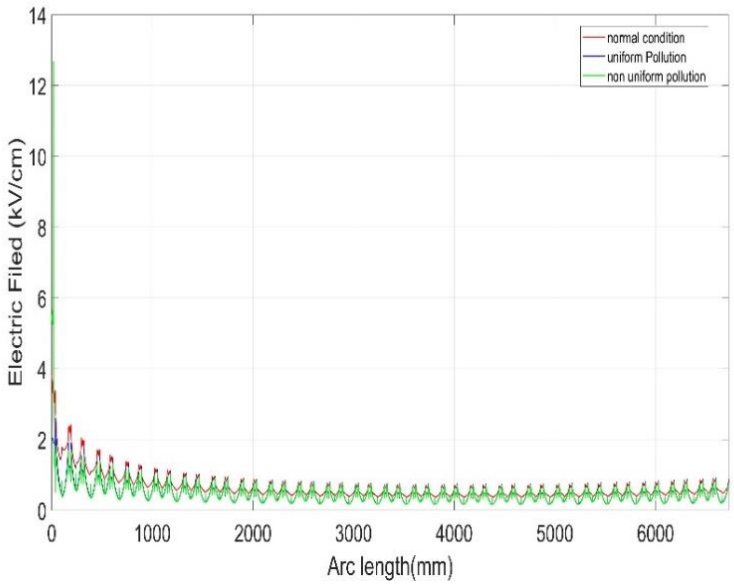

Figure 19: Comparative analysis of electric field for normal condition, uniform pollution and non-uniform pollution

At the start of the arc length i.e. near triple junction point, there is a significant peak in the electric field intensity for all conditions. But the peak is most pronounced, reaching around 12.683 kV/cm, indicating a higher concentration of the electric field near the energized end of the insulator for non-uniform pollution condition shown by green line. The red line representing the electric field distribution under normal conditions (without any pollution) shows a moderately high electric field at the beginning i.e. 3.932 kV/cm, which quickly drops and stabilizes as the arc length increases. For the uniform pollution, shown by blue line the electric field initially follows a similar trend to the normal condition, with a comparatively low peak at the start i.e. 2.629 kV/cm so the electric field influence gets reduced by the pollution layer. Therefore, compared to the discontinuous contamination a uniform contamination of the insulator is more beneficial for the insulator [21]. The electric field distribution under non-uniformly polluted conditions starts with an extremely high peak and exhibits greater and more irregular fluctuations along the entire length of the insulator. This indicates that non-uniform pollution results in high electric field stress compared to both normal and uniformly polluted conditions, likely due to the variation of different level of permittivity's at the insulator's surface.

3.5.3 Electric Field Distribution with recommended and optimized corona ring under non uniform pollution condition

Figure 20 compares the electric field distribution for recommended and optimized corona rings in the presence of non-uniform pollution.

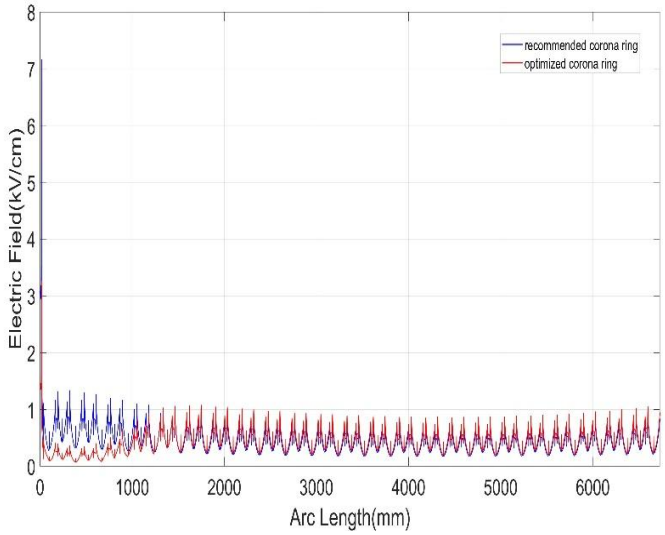

Figure 20: Comparative analysis of electric field for recommended and optimized corona ring in presence of non-uniform pollution

As the non-uniform pollution results in a more uneven electric field distribution compared to both normal and uniformly polluted conditions with a peak value of 12.683 kV/cm. So, during the non-uniform pollution condition it is very much necessary to minimize the electric field as much as possible. At the beginning of the arc length (near triple junction point), there is a noticeable spike in the electric field for both corona ring configurations. However, the electric field for the "recommended corona ring" represented by blue curve is significantly higher compared to the "optimized corona ring" represented by red curve. The peak electric field value for the recommended configuration reaches around 7.166 kV/cm, whereas the optimized configuration peaks at a lower value of approximately 3.262 kV/cm. This suggests that the optimized corona ring design effectively reduces the maximum electric field intensity at the triple junction point of the insulator. However, with the optimized corona along the insulator the electric field slightly increases as compared to that of recommended corona ring.

4. Conclusions

In this paper we optimized a corona ring for 230 kV polymeric insulator using FEM and different optimization techniques. Initially FEM was carried out to study the electric field behavior of insulator and based on the results corona ring parameters were studied to develop the objective function of electric field at triple junction point with respect to corona ring parameters. Second order polynomial equation was obtained as objective function which when optimized with different optimization techniques gave same result for optimized corona ring parameters.

The result shows that at triple junction point with the installation of optimized corona ring the electric field strength at the triple junction point was 0.8423 kV/cm i.e., 58.85% reduction as compared to that of recommended corona ring. The installation of optimized corona ring shifts the maximum electric field away from the triple junction point and the electric field strength across the insulator is slightly higher compared to that of recommended corona ring. Addition of uniform pollution layer reduces the contribution of the electric field near the triple junction point whereas addition of non-uniform pollution layer heavily increases the electric field stress near the triple junction point resulting the electric field to be 12.683 kV/cm i.e. 222.558 % increment compared to normal condition (without pollution layer). For the non-uniform pollution condition, the presence of recommended corona ring reduces the electric field to 7.166 kV/cm i.e., 43.5% reduction and the presence of optimized corona ring reduces the electric field to 3.262 kV/cm i.e., 74.28% reduction which is less than 4.2 kV/cm (electric field strength that should not surpass). Therefore, the optimized corona ring reduces the electric filed stress by 54.48% compared to recommended corona ring in presence of non-uniform pollution. However, the optimal design of corona ring should consider the mechanical, economical constraints and the material used to build up the corona ring which can be analyzed in future works.

Conflicts of interest statement

The authors declare no conflicts of interest for this study.

Data availability statement

The data that support the findings of this study are available from the corresponding author upon reasonable request.

References

1. E. Akbari, M. Mirzaie, A. Rahimnejad, and M. B. Asadpoor, "Finite element analysis of disc insulator type and corona ring effect on electric field distribution over 230-kV insulator strings," *International Journal of Engineering and Technology*, vol. 1, no. 4, pp. 407–419, 2012.
2. W. L. Vosloo, R. E. Macey, and C. de Tourreil, *The Practical Guide to Outdoor High Voltage Insulators*, Crown Publications, 2008.
3. E. A. Murawwi and A. El-Hag, "Corona ring design for a 400 kV non-ceramic insulator," in *2011 2nd International Conference on Electric Power and Energy Conversion Systems (EPECS)*, Sharjah, United Arab Emirates, 2011, pp. 1–4, doi: 10.1109/EPECS.2011.6126818.
4. H. Benguesmia, N. M'ziou, and A. Boubakeur, "Simulation of the potential and electric field distribution on high voltage insulator using the finite element method," *Diagnostyka*, vol. 19, no. 2, pp. 41–52, 2018.
5. E. Akbari, M. Mirzaie, A. Rahimnejad, and M. B. Asadpoor, "Finite element analysis of disc insulator type and corona ring effect on electric field distribution over 230-kV insulator strings," *International Journal of Engineering and Technology*, vol. 1, no. 4, pp. 407–419, 2012.

6. L. Cui and M. Ramesh, "Prediction of flashover voltage using electric field measurement on clean and polluted insulators," *International Journal of Electrical Power & Energy Systems*, vol. 116, 2020.
7. Q.-y. Xu and Y.-s. Zhu, "Research on corona ring setting and structure optimization of composite insulator based on neural network," in *Proc. 2nd Int. Conf. Artificial Intelligence, Management Science and Electronic Commerce (AIMSEC)*, Deng Feng, China, 2011, pp. 4224–4227.
8. D. Azizi, A. Gholami, and A. Siadatan, "Corona ring optimization for different cases of polymer insulators based on its size and distance," *Journal of Artificial Intelligence and Electrical Engineering*, vol. 1, no. 2, 2012.
9. D. Cruz Domínguez, F. P. Espino-Cortés, P. Gómez, and U. C. Adolfo López Mateos Lindavista, "Optimized design of electric field grading systems in 115 kV non-ceramic insulators," *IEEE Transactions on Dielectrics and Electrical Insulation*, vol. 20, no. 1, pp. 63–70, 2013.
10. D. Doufene, S. Bouazabia, A. A. Ladjici, and A. Haddad, "Polluted insulator optimization using neural network combined with genetic algorithms," in *Proc. 18th Int. Symp. Electromagnetic Fields Mechatronics, Electr. Electron. Eng. (ISEF)*, Lodz, Poland, 2017, pp. 1–2.
11. B. M'Hamdi, Y. Benmahamed, M. Teguar, I. B. M. Taha, and S. S. M. Ghoneim, "Multi-objective optimization of 400 kV composite insulator corona ring design," *IEEE Access*, vol. 10, pp. 27579–27590, 2022.
12. W. Sima, F. P. Espino-Cortes, E. A. Cherney, and S. H. Jayaram, "Optimization of corona ring design for long-rod insulators using FEM based computational analysis," in *Conf. Record 2004 IEEE Int. Symp. Electr. Insul.*, Indianapolis, IN, USA, 2004, pp. 480–483.
13. J. Ndoumbe, E. T. Nkouetcha, and J. G. O. Emboueme, "FEM analysis of the electric field and potential of various types of insulators under uniform pollution," *International Journal of Research and Review*, vol. 10, no. 8, Aug. 2023.
14. J. A. Diaz-Acevedo, A. Escobar, and L. F. Grisales-Noreña, "Optimization of corona ring for 230 kV polymeric insulator based on finite element method and PSO algorithm," *Electric Power Systems Research*, vol. 201, Dec. 2021, doi: 10.1016/j.epsr.2021.107521.
15. M. S. Naidu and V. Kamaraju, *High Voltage Engineering*, 5th ed., McGraw Hill Education (India) Private Limited, 2013.
16. M. Jain, V. Saihjpal, N. Singh, and S. B. Singh, "An overview of variants and advancements of PSO algorithm," *Applied Sciences*, vol. 12, no. 17, p. 8392, Aug. 2022, doi: 10.3390/app12178392.
17. ResearchGate.[Online].Available:https://www.researchgate.net/figure/Flowchart-for-basic-PSO-algorithm_fig3_266614526. [Accessed: Sep. 6, 2024].
18. MathWorks,[Online].Available:https://www.mathworks.com/help/optim/ug/choosing-the-algorithm.html. [Accessed: Sep. 6, 2024].
19. A. Ahmadianfar, A. A. Heidari, A. H. Gandomi, X. Chu, and H. Chen, "RUN beyond the metaphor: An efficient optimization algorithm based on Runge Kutta method," *Expert Systems with Applications*, vol. 181, p. 115079, 2021, doi: 10.1016/j.eswa.2021.115079.

20. K. Belhouchet, A. Zemmit, A. Bayadi, L. Ouchen, and A. Zorig, "A novel application of artificial intelligence technology for outdoor high-voltage composite insulator," *Measurement*, vol. 238, 2024, Art. no. 115372.
21. J. Ndoumbe, E. T. Nkouetcha, and J. G. Ologo Emboueme, "FEM analysis of the electric field and potential of various types of insulators under uniform pollution," *International Journal of Research and Review*, vol. 10, no. 8, pp. 1061–1068, Sep. 2023, doi: 10.52403/ijrr.202308134.